THE JOURNAL OF BIOLOGICAL CHEMISTRY VOL. 290, NO. 44, pp. 26821–26831, October 30, 2015

Dimerization-dependent Folding Underlies Assembly Control of the Clonotypic αβT Cell Receptor Chains*

Received for publication, September 1, 2015, and in revised form, September 21, 2015 Published, JBC Papers in Press, September 23, 2015, DOI 10.1074/jbc.M115.689471

Matthias J. Feige[‡1], **Julia Behnke**[‡2], **Tanja Mittag**[§3], **and Linda M. Hendershot**[‡4]

From the Departments of [‡]*Tumor Cell Biology and* [§]*Structural Biology, St. Jude Children's Research Hospital, Memphis, Tennessee 38105*

Background: Assembly of heteromeric membrane protein complexes is monitored prior to their transport to the cell surface.
Results: Each of the αβTCR clonotypic chains comprises one domain that folds upon assembly.
Conclusion: Proper αβTCR biogenesis is scrutinized by assembly-coupled folding steps.
Significance: This study shows how the assembly of heteromeric membrane proteins can be monitored and indicates limitations of the possible T cell repertoire.

In eukaryotic cells, secretory pathway proteins must pass stringent quality control checkpoints before exiting the endoplasmic reticulum (ER). Acquisition of native structure is generally considered to be the most important prerequisite for ER exit. However, structurally detailed protein folding studies in the ER are few. Furthermore, aberrant ER quality control decisions are associated with a large and increasing number of human diseases, highlighting the need for more detailed studies on the molecular determinants that result in proteins being either secreted or retained. Here we used the clonotypic αβ chains of the T cell receptor (TCR) as a model to analyze lumenal determinants of ER quality control with a particular emphasis on how proper assembly of oligomeric proteins can be monitored in the ER. A combination of *in vitro* and *in vivo* approaches allowed us to provide a detailed model for αβTCR assembly control in the cell. We found that folding of the TCR α chain constant domain Cα is dependent on αβ heterodimerization. Furthermore, our data show that some variable regions associated with either chain can remain incompletely folded until chain pairing occurs. Together, these data argue for template-assisted folding at more than one point in the TCR α/β assembly process, which allows specific recognition of unassembled clonotypic chains by the ER chaperone machinery and, therefore, reliable quality control of this important immune receptor. Additionally, it highlights an unreported possible limitation in the α and β chain combinations that comprise the T cell repertoire.

In eukaryotic cells, proteins of the secretory pathway are produced in the endoplasmic reticulum (ER).[5] In higher eukaryotes, these proteins usually enter the ER co-translationally as unfolded polypeptide chains and must acquire their native structure before traversing further along the secretory pathway. This often includes formation of disulfide bonds and glycosylation as well as subunit assembly, processes that are aided and scrutinized by a comprehensive ER-resident protein folding and quality control (QC) machinery (1, 2). To avoid detrimental effects to the organism, the cell has to distinguish between native proteins, partially folded proteins, and ones that are unable to fold. However, in some cases, this discrimination fails, allowing either the ER exit of potentially harmful molecules or the degradation of proteins that could perform their biological functions (3, 4). Therefore, which features of partially folded or incompletely assembled proteins the ERQC machinery recognizes is a key question. Shortcomings in our understanding are partially due to the limited resolution with which protein folding can be monitored in the cell (5, 6).

To provide molecular insights into processes of ERQC, we focused on the α and β chains of the T cell receptor (TCR). The αβTCR is a longstanding model for the quality control of oligomeric membrane proteins, and a great deal is understood about cellular checkpoints in its assembly (7–15). It is composed of eight polypeptide chains, the clonotypic α and β chains and the invariant co-receptor chains (CD3γ, δ, ε, and ζ; Fig. 1*A*), all of which must assemble correctly for the αβTCR to

* This work was supported by National Institutes of Health Grants R03 AI097733 and R01 GM54068 (to L. M. H.) and by the American Lebanese Syrian Associated Charities of St. Jude Children's Research Hospital. The authors declare that they have no conflicts of interest with the contents of this article.

[1] A Rudolf Mößbauer tenure track professor cofinanced through the Marie Curie COFUND program. Supported by the German Academy of Sciences Leopoldina Grant LPDS 2009-32, the Paul Barrett endowed fellowship of St. Jude Children's Research Hospital, the Center for Integrated Protein Science Munich, and the Technische Universität München Institute for Advanced Study funded by the German Excellence Initiative and the European Union Seventh Framework Programme under Grant Agreement 291763. To whom correspondence may be addressed: Center for Integrated Protein Science at the Dept. of Chemistry and Institute for Advanced Study, Technische Universität München, Lichtenbergstr. 2a, 85748 Garching, Germany. Tel.: 49-89-289-10595; Fax: 49-89-289-10698; E-mail: matthias.feige@tum.de.

[2] Present address: MorphoSys AG, Lena-Christ-Str. 48, 82152 Martinsried/Planegg, Germany. Supported by a Boehringer Ingelheim Ph.D. scholarship.

[3] Supported by a V Foundation scholar grant.

[4] To whom correspondence may be addressed: Dept. of Tumor Cell Biology, St. Jude Children's Research Hospital, 262 Danny Thomas Pl., Memphis, TN 38105. Tel.: 901-595-2475; Fax: 901-595-2381; E-mail: linda.hendershot@stjude.org.

[5] The abbreviations used are: ER, endoplasmic reticulum; QC, quality control; TCR, T cell receptor; Cnx, Calnexin; Crt, Calreticulin; LC, light chain; HC, heavy chain; TM, transmembrane; TROSY, transverse relaxation optimized spectroscopy; HSQC, heteronuclear single quantum coherence.

be transported to the cell surface (16–18). First, the α and β chains pair with their designate CD3 co-receptor subunits, giving rise to α-CD3δε and β-CD3γε trimers, respectively (19). In each case, complementary basic/acidic residues in the transmembrane segments of these chains guide assembly of the trimers and, as has been dissected in detail for the α chains, provide a means to identify chains that do not assemble with CD3 components (7, 8, 10, 12, 20). Retention motifs in the CD3 subunits appear to play an important role in the final step of αβTCR assembly: interaction of αβ-CD3γδε$_2$ hexamers with ζ_2 homodimers to form the complete αβTCR (21, 22). However, it has remained unclear how assembly of the two α-CD3δε and β-CD3γε trimers is monitored and what role the various lumenal domains of the clonotypic αβ chains play in ERQC. Combining the individual strengths of *in vitro* and *in vivo* experimental approaches, we set out to study the molecular events occurring upon heterodimerization of the TCR α/β chains with a view to deriving general insights into how the ERQC system monitors protein assembly.

Experimental Procedures

Protein Production and Purification—For *in vitro* studies, individual constructs were amplified from synthetic TCR genes optimized for *Escherichia coli* expression (Geneart, Regensburg, Germany) and cloned into the pET28a expression vector (Novagen, Gibbstown, NJ). Expression of the various constructs was performed overnight at 37 °C, and resulted in inclusion bodies. Inclusion bodies were solubilized in 100 mM Tris/HCl (pH 8.0), 10 mM EDTA, 10 mM β-mercaptoethanol, and 8 M urea. Solubilized inclusion bodies were centrifuged (20,000 × *g*, 30 min, 10 °C). The supernatant was applied to a Q-Sepharose column equilibrated in 100 mM Tris/HCl (pH 8.0), 10 mM EDTA, and 5 M urea. Subsequently, the flowthrough was applied to an SP-Sepharose column equilibrated in the same buffer. None of the proteins of interest bound to either column. Accordingly, the flowthrough of the SP-Sepharose column was collected and dialyzed overnight against 100 mM Tris/HCl (pH 8.0), 3 M guanidinium chloride, 5 mM EDTA, and 1 mM DTT. Subsequently, the proteins were applied to a Superdex 200pg (26/60) gel filtration column (GE Healthcare) equilibrated in the same buffer. Proteins were then diluted to 0.1 mg/ml in 250 mM Tris/HCl (pH 8.0), 250 mM L-arginine, 5 mM EDTA, 0.25 mM GSSG, and 0.25 mM GSH and refolded overnight at 4 °C via dialysis against the same buffer. The refolded proteins were concentrated and applied to a Superdex 200pg (26/60) gel filtration column equilibrated in PBS and, if necessary, additionally to a Superdex200 10/300 GL HPLC column (GE Healthcare) equilibrated in PBS. All plasmids were sequenced, and protein identities were verified by mass spectrometry. For NMR samples, proteins were expressed in M9 minimal medium containing ^{15}N-labeled ammonium chloride.

Spectroscopic Techniques—All CD spectra were recorded with a Jasco J-710 spectropolarimeter (Jasco, Grossumstadt, Germany) at 25 °C in PBS in 0.2-mm quartz cuvettes at a protein concentration of 35 μM. Spectra were recorded 16 times, averaged, and buffer-corrected. Gradient-selected ^{1}H-^{15}N TROSY HSQC spectra of samples in PBS and 90% H_2O/10% D_2O were recorded at 298 K on a Bruker Avance 800 MHz NMR spectrometer with a TCI triple-resonance cryogenic probe with 1024 × 128 complex data points and varying number of scans to account for the different protein concentrations and sensitivity. Spectra were processed with nmrPipe (23).

Assessment of Disulfide Bridge Formation—To monitor disulfide bridge formation between and within different proteins *in vitro*, the respective proteins were (co-)incubated at 25 °C in PBS supplemented with 1 mM GSH/GSSG each. The concentration of each protein was 35 μM. After 3 h, samples were supplemented with 20 mM *N*-ethylmaleimide and Laemmli buffer (with or without β-mercaptoethanol) and boiled for 3 min. Proteins were separated on 14% SDS-PAGE gels.

Partial Proteolysis and Mass Spectrometry—Stability against proteolytic digestion was assessed by partial proteolysis experiments. Before the addition of protease, proteins were (co-)incubated for 3 h at 25 °C in PBS at a protein concentration of 35 μM each. If present, GSH and GSSG were used at a concentration of 1 mM each, and any reduction/oxidation reactions were quenched by the addition of 20 mM *N*-ethylmaleimide prior to addition of the protease. After the preincubation step, trypsin (Trypsin Gold, Promega, Madison, WI) was added at a concentration of 1:80 (w/w). Aliquots were withdrawn after different time points, and the proteolysis was terminated by the addition of Roche complete protease inhibitor without EDTA (Roche Applied Science) and Laemmli buffer (without β-mercaptoethanol) and boiling for 3 min. Proteins were separated on 14% SDS-PAGE gels. Gels were quantified with ImageQuant TL software (GE Healthcare). Mass spectrometry experiments were performed by the St. Jude Proteomics core facility using tryptic digestion combined with LC-MS/MS.

Cell Culture Experiments—Constructs were either amplified from synthetic TCR genes optimized for human expression (A6 TCR) (Geneart) or from synthetic genes with the authentic cDNA sequence of the proteins (HA TCR) and cloned into the pSVL vector. BiP was used in a pMT vector (24). All sequences were verified. Experiments were performed in COS-1 cells that were grown in DMEM supplemented with 10% (v/v) fetal bovine serum, 2 mM L-glutamine, and a 1% (v/v) antibiotic-antimycotic solution (25 μg/ml amphotericin B, 10,000 μg/ml streptomycin, and 10,000 units of penicillin; Cellgro/Mediatech, Manassas, VA) (complete DMEM) at 37 °C and 3% CO_2. COS-1 transfections were carried out for 24 h in p60 dishes using GeneCellin (BioCellChallenge, Toulon, France) according to the protocol of the manufacturer. For metabolic labeling, cells were starved for 30 min in complete DMEM without Met and Cys and subsequently supplemented with 100 μCi/p60 dish of EasyTag^{TM} EXPRESS35S protein labeling mixture (PerkinElmer Life Sciences), with labeling times indicated in the respective figures. Labeling was carried out in the presence of 10 mM DTT for DTT washout experiments. Prior to lysis, cells were washed twice in ice-cold PBS supplemented with 20 mM *N*-ethylmaleimide when samples were to be run on non-reducing SDS-PAGE gels. Cells were lysed with radio-immunoprecipitation assay buffer (50 mM Tris/HCl (pH 7.5), 150 mM NaCl, 1.0% Nonidet P40 substitute, 0.5% sodium deoxycholate, 0.1% SDS, 0.1 mM PMSF, and 1× Roche complete protease inhibitor without EDTA) or Nonidet P-40 lysis buffer in the case of chaperone co-immunoprecipitation experiments (50

mM Tris/HCl (pH 7.5), 150 mM NaCl, 0.5% Nonidet P40 substitute, 0.5% sodium deoxycholate, 0.1 mM PMSF, and 1× Roche complete protease inhibitor without EDTA, supplemented with 10 units/ml Apyrase for BiP interaction studies (Sigma-Aldrich, St. Louis, MO)). Immunoprecipitations were performed with antibodies against the TCR Cα domain (TCR1145) or Cβ domain (TCR1151) (Thermo Fisher Scientific, Rockford, IL), the FLAG tag (F7425, Sigma), BiP (25), or the HA tag (produced in our laboratory). 3 μg of antibody or 3 μl of serum were used for each cell lysate of one p60 dish and rotated overnight at 4 °C, and, subsequently, CaptivA™ PriMAB protein A-agarose (Repligen Bioprocessing, Waltham, MA) was added for 2 h at 4 °C under rotation. Immunoprecipitated proteins were washed three times with radio-immunoprecipitation assay buffer or Nonidet P-40 washing buffer (for chaperone co-immunoprecipitations 50 mM Tris/HCl (pH 7.5), 400 mM NaCl, 0.5% Nonidet P40 substitute, and 0.5% sodium deoxycholate) and eluted with Laemmli buffer for 5 min at 95 °C. For Endo H/PNGase F (New England Biolabs, Ipswich, MA) deglycosylation experiments, proteins were eluted with glycoprotein-denaturing buffer and subsequently treated according to the protocols of the manufacturer. For pulse-chase experiments, cells were washed twice with ice-cold PBS after the labeling step, and then complete DMEM supplemented with additional 2 mM of cold Cys and Met was added for the chase times indicated in the figures.

Results

Heterodimerization of the TCR α and β Chains Is a Prerequisite for ER Exit—To provide insights into the assembly process of the clonotypic TCR α- and β-chains, we used the structurally well characterized human A6 αβTCR (26, 27). Experiments were performed in COS-1 cells, which allow for complete TCR assembly and transport (28). Because this study focused on quality control steps that monitor assembly of the TCR α/β chains, the membrane-integrated basic residues of these chains (Fig. 1*A*) were mutated to Leu (designated $\alpha^{RK->LL}$ and $\beta^{K->L}$, respectively). This allows stable membrane integration of the TCR α chain in the absence of CD3 assembly (10, 29) and, therefore, permitted us to focus on the quality control checkpoints for the clonotypic TCR α/β chains downstream of this critical step.

The fate of $\alpha^{RK->LL}$ and $\beta^{K->L}$ was monitored by pulse-chase metabolic labeling experiments in which neither $\alpha^{RK->LL}$ nor $\beta^{K->L}$ acquired Endo H resistance during a 3-h chase, indicative of their retention in the ER (Fig. 1*B*, *top panel*). In contrast, when $\alpha^{RK->LL}$ and $\beta^{K->L}$ were co-expressed, α chains could be co-precipitated with anti-Cβ antibodies (Fig. 1*B*, *bottom panel*, *black asterisk*), and an Endo H-resistant, PNGase F-sensitive species was observed after the chase (Fig. 1*B*, *bottom panel*, *red asterisk*), an indication of further sugar modification in the Golgi. When analyzed under non-reducing conditions, the formation of an αβ heterodimer was evident (Fig. 1*C*, *black arrow*). This heterodimer became larger in size over time, also suggesting further glycan modification in the Golgi (Fig. 1*C*, *red arrow*). Therefore, when their basic transmembrane (TM) residues are mutated and CD3 co-receptor interactions are abolished, the clonotypic TCR α and β chains are retained in the ER when unassembled and can continue to the Golgi upon heterodimerization. This indicates retention motifs that become inactive upon heterodimerization, which are different from the intramembrane basic residues or CD3 association.

The ER Chaperones Calnexin and BiP Recognize Unassembled TCR α and β Chains—As glycoproteins, the TCR α and β chains are substrates of the ER Calnexin (Cnx)/Calreticulin (Crt) lectin chaperone system (30, 31). The action of Cnx, however, seems to be limited to early stages of αβTCR biogenesis (32) and is not essential for the correct assembly of αβTCRs (33). Additionally, the ER Hsp70 orthologue BiP (10, 34) and the ER lumenal large Hsp70 Grp170 (35) bind to TCR α and β chains. The precise role of these chaperones in TCR assembly and their binding sites within the clonotypic TCR chains have remained unclear.

When chaperone interactions were analyzed, we observed stable interaction of Cnx with unassembled α and β chains (Fig. 2*A*). These interactions were reduced significantly when proteins devoid of their TM regions were analyzed (Fig. 2*B*). Interaction with the ER-lumenal lectin chaperone Crt was significantly less pronounced and not even detectable for the α chain (Fig. 2, *A* and *B*), in agreement with earlier studies (30). The α and β chains can each be structurally divided into two Ig-like ectopic domains (Vα and Cα or Vβ and Cβ, respectively), a flexible stalk that connects the constant domains to the TM regions, the TM regions themselves, and a short cytoplasmic tail (Fig. 2*C*). To assess the role of these different elements in Cnx interaction and ERQC, we created mutants of $\alpha^{RK->LL}$ and $\beta^{K->L}$ where we individually replaced either the flexible stalk or the cytoplasmic tail with poly-GS sequences of similar length (denoted as $\alpha^{RK->LL/stalk->GS}$ and $\alpha^{RK->LL/tail->GS}$ or $\beta^{K->L/stalk->GS}$ and $\beta^{K->L/tail->GS}$, respectively). None of these mutants became Endo H-resistant over a chase period of 5 h, and all mutants showed similar half-lives (Fig. 2, *D* and *E*) and wild-type-like interaction with Cnx (Fig. 2*F*), arguing that the lumenal domains themselves are key factors in ERQC.

Next we analyzed how the other major chaperone system of the ER, the Hsp70 system centered around BiP (36), recognized the TCR α and β chains. In agreement with data published previously (10, 34, 35) we found both $\alpha^{RK->LL}$ and $\beta^{K->L}$ to be BiP substrates (Fig. 3*A*). Constructs devoid of their TM regions ($\alpha^{\Delta TM}$ or $\beta^{\Delta TM}$, respectively; Fig. 1*A*) showed interactions with BiP that were comparable with their membrane-integrated counterparts (Fig. 3*A*), revealing the presence of BiP-binding sites within the ectodomains of both the TCR α and β chains. Conversely, Cnx interactions were reduced significantly when proteins devoid of their TM regions were analyzed (Fig. 2, *A* and *B*), indicating that membrane proximity or the TM regions themselves are important for the interaction of TCR α/β chains with the integral membrane protein Cnx (37, 38). To further dissect BiP interactions with the TCR clients, we individually analyzed its interaction with each of the isolated α/β chain domains. We reproducibly observed binding, albeit weak, of BiP to the α chain Cα domain but essentially no binding to Vα (Fig. 3*B*). The opposite was true in the case of the β chain. The Vβ domain bound to BiP very strongly, whereas we observed very minimal interaction of Cβ with BiP (Fig. 3*B*). Of note, BiP preferentially bound the less glycosylated form of the β chain

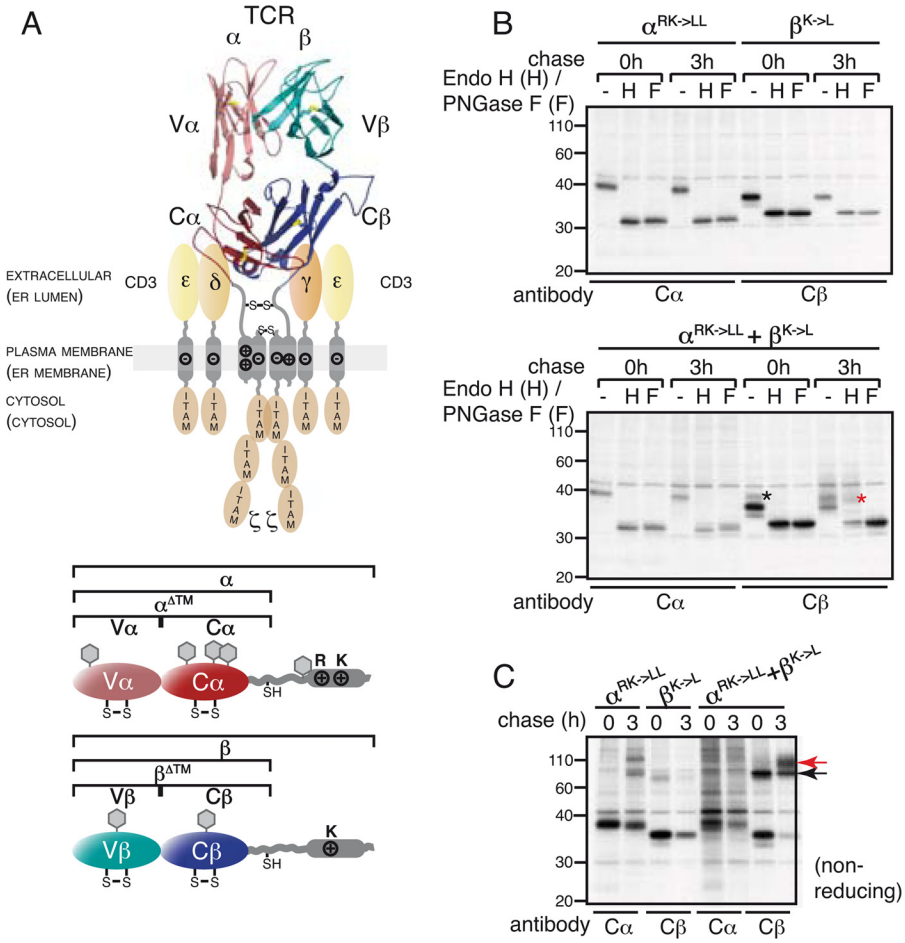

FIGURE 1. **Assembly of the TCR α and β chains is a prerequisite for ER exit.** *A*, the αβTCR is composed of two clonotypic chains (α and β, structure on the basis of PDB code 1QSE), the invariable CD3 co-receptor ($\gamma\delta\varepsilon_2$), and the ζ dimer (*ITAM:* immunoreceptor tyrosine-based activation motif). The clonotypic chains comprise one variable (Vα and Vβ, respectively) and one constant domain each (Cα and Cβ, respectively). Intradomain disulfide bonds are shown in *yellow*. Final dispositions of the various domains and during biosynthesis (in *parentheses*) are indicated. TM basic (+) and acidic residues (−) are shown. A flexible stalk connects the TM regions with the constant domains. In the complete receptor, the α and β chains are linked via a disulfide bridge in the stalk region. The constructs used in this study are shown in the *bottom panel*. Cysteines/disulfide bridges and predicted glycosylation sites (N*X*S/T sequences (*X* ≠ Pro), *gray hexagons*) are indicated. *B*, pulse-chase experiments on the isolated (*top panel*) or co-expressed (*bottom panel*) α and β chains devoid of their TM basic residues ($\alpha^{RK->LL}$ and $\beta^{K->L}$, respectively). Only the Cβ antibody is able to immunoprecipitate the αβ heterodimer (the co-precipitating α chain is marked with a *black asterisk*). Where indicated, proteins were deglycosylated with Endo H or PNGase F. A *red asterisk* indicates the Endo H-resistant species. Chase times are shown above the lanes. 2.5 μg of each α chain construct and 1.5 μg of each β chain construct were (co-)transfected, and COS-1 cells were metabolically labeled for 1 h. *C*, pulse-chase experiments were performed as in *B*, except that the samples were analyzed under non-reducing conditions. The *black arrow* indicates the αβ-heterodimer, whereas its Golgi-modified form is marked with a *red arrow*.

(Fig. 3, *A* and *B*), whereas Cnx did not show such a preference (Fig. 2*A*). The absence of glycosylation may facilitate BiP binding by exposing binding sites or because of the absence of competition with lectin chaperone binding (37–39).

The Isolated TCR α and β Chains Contain Incompletely Folded Domains—To understand the observed chaperone binding characteristics in more structural detail, we assessed the folding status of the α/β chains and their individual domains in the ER by monitoring intradomain disulfide bond formation in the various α/β chain constructs. To do so, cells were treated with DTT during metabolic labeling to inhibit the formation of disulfide bonds in newly synthesized proteins. Subsequent reculturing in DTT-free media allows oxidation to occur. The presence of a disulfide bond can lead to a more compact state of a protein unfolded in SDS, which may be detected by a modest increase in its mobility on non-reducing SDS-PAGE gels (40). If native disulfide bonds do not form, then it is a clear indication of incomplete folding, whereas, if oxidation occurs, this most often correlates with folding. The α and β chains ran slightly faster on non-reducing SDS-PAGE gels after the removal of DTT (Fig. 4*A*), indicative of the formation of at least one intradomain disulfide bond. The shift was very small, however, likely because of the large size of the proteins, and it was more readily detectable for constructs devoid of their TM regions (Fig. 4*A*). When the individual domains were assessed similarly, Vα and both bands of Cβ, which correspond to different glycospecies, showed increased mobility on non-reducing gels after removal of DTT, indicative of oxidative folding. In contrast, Cα had an unaltered mobility, and Vβ actually migrated slightly slower, arguing neither of these domains formed an internal disulfide bond (Fig. 4*A*). Therefore, in agreement with our BiP binding data, the isolated Cα and Vβ domains appeared to remain incompletely folded.

Genetic recombination and selection give rise to a different set of variable domains in each TCR, which might affect their

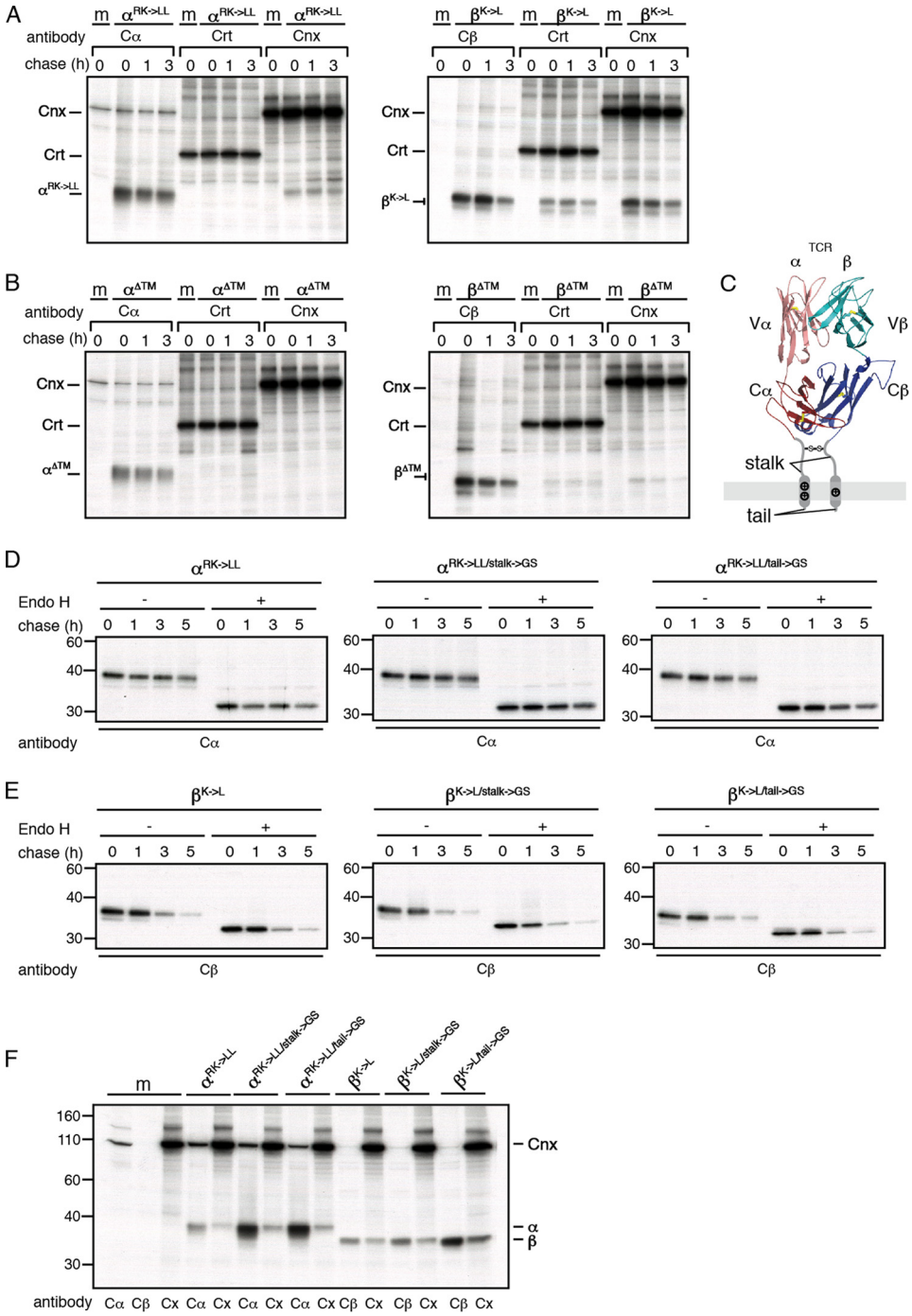

FIGURE 2. **Cnx/Crt interactions and maturation of the TCR α/β chains *in vivo*.** *A*, to analyze interactions of $\alpha^{RK->LL}$ and $\beta^{K->L}$ with endogenous Crt and Cnx, COS-1 cells were transfected with 4 μg of each TCR construct, metabolically labeled for 16 h, and chased for the indicated times. Lysates were immunoprecipitated with the indicated antibodies, and their association with the lectin chaperones is indicated. *m*, mock. *B*, the same as in *A*, except that constructs devoid of their TM regions ($\alpha^{\Delta TM}$ and $\beta^{\Delta TM}$) were used. *C*, schematic of the αβTCR with the flexible stalks, TM basic residues, and cytoplasmic tails indicated. *D*, to assess the impact of the flexible stalk and the cytoplasmic tail on ER retention of the TCR α chain, COS-1 cells were transfected with the indicated α chain constructs, metabolically labeled for 1 h, and subsequently either lysed directly or chased for the indicated times. Where indicated, proteins were treated with Endo H. *E*, experiments similar to those described in *D* were conducted for the TCR β chain. *F*, influence of the stalk or the cytoplasmic tail on the interaction of either the TCR α chain or the β chain with Cnx. The antibodies used for immunoprecipitation are indicated below the gel (the anti-Cnx antibody is denoted with *Cx*). Note that the Cα antibody precipitates an unspecific band the size of Cnx, which is also observed in cells transfected with empty pSVL vector (*m*, mock). 4 μg of each construct were transfected.

folding, whereas Cα and Cβ are conserved between different αβTCRs. We therefore assessed the folding properties of the Vα and Vβ domains derived from another, anti-HA human αβTCR (41). Interestingly, for the anti-HA αβTCR, the Vα domain seemed to be unable to form its disulfide bond, whereas Vβ showed a small shift upon DTT washout, indicative of it forming an intradomain disulfide bond (Fig. 4*B*). Furthermore, in contrast to the A6 Vα domain, the HA TCR Vα domain strongly bound to BiP (compare Figs. 3*B* and 4*C*), whereas binding of the HA Vβ domain was of similar strength as that

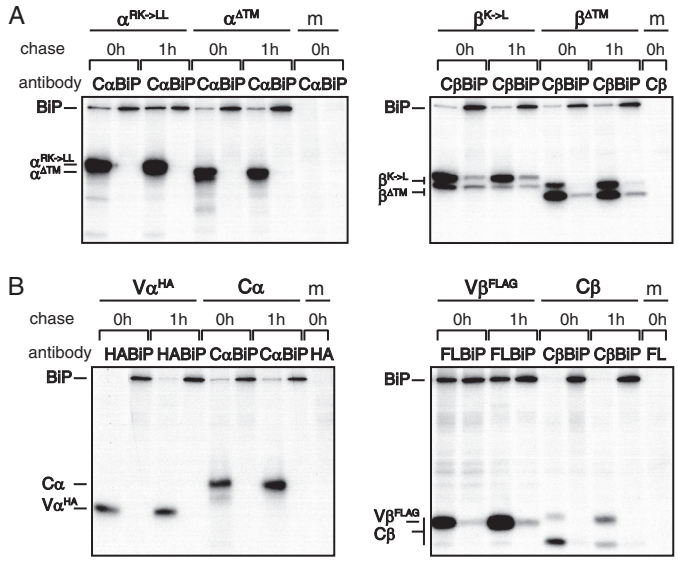

FIGURE 3. **Interactions of the TCR α/β chains and domains with BiP *in vivo*.** *A*, association of BiP with the A6 TCR α and β chains in the presence ($\alpha^{RK->LL}$ or $\beta^{K->L}$, respectively) or absence of their TM regions ($\alpha^{\Delta TM}$ or $\beta^{\Delta TM}$, respectively) was detected by co-immunoprecipitation. 3 μg of the TCR constructs were co-transfected with 2 μg of BiP. Cells were metabolically labeled for 30 min. Chase times and precipitating antibodies are indicated. *m*, mock transfection. *B*, BiP binding experiments for the individual A6 TCR α and β chain domains were performed as in *A*. Variable domains were epitope-tagged as indicated. The two bands observed for the β chain/Cβ domain represent two glycospecies (56).

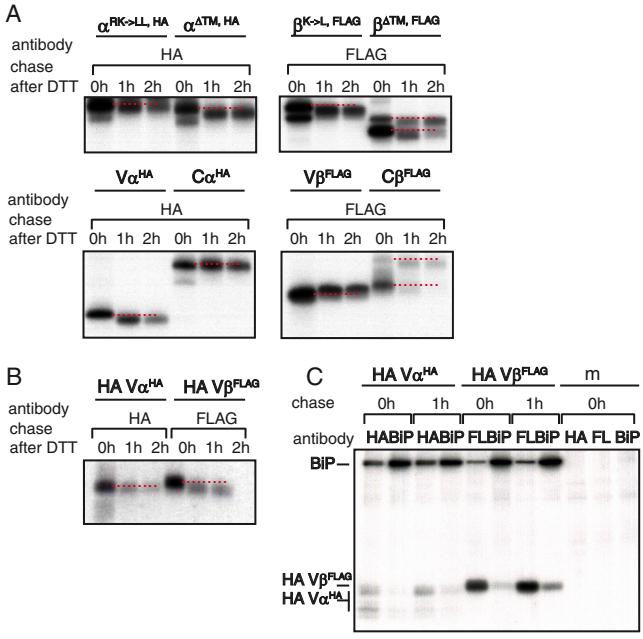

FIGURE 4. **Redox states of the TCR α/β chains and domains *in vivo* and chaperone interactions of the HA TCR.** *A*, DTT washout experiments were conducted for the α and β chains in the presence ($\alpha^{RK->LL}$ or $\beta^{K->L}$, respectively) or absence of their TM regions ($\alpha^{\Delta TM}$ or $\beta^{\Delta TM}$, respectively) and their constituent domains. Experiments were performed in COS-1 cells using epitope-tagged constructs (HA or FLAG) to allow immunoprecipitation of all redox species. COS-1 cells were transfected with 4 μg of each TCR construct, metabolically labeled in the presence of 10 mM DTT for 30 min, and subsequently either lysed directly or washed to remove DTT and recultured in complete medium for the indicated times. Immunoprecipitated proteins were analyzed by non-reducing SDS-PAGE. To guide the eye, *horizontal dotted red lines* are shown at the positions of the reduced species. *B*, experiments similar to those in *A* were performed for the anti-HA TCR variable domains. The two bands observed for the HA Vα domain correspond to two glycospecies. *C*, BiP binding experiments were performed for the anti-HA TCR variable domains. 3 μg of the TCR constructs were co-transfected with 2 μg of BiP. Cells were metabolically labeled for 30 min. Chase times and precipitating antibodies are indicated. *m*, mock transfection.

observed for the A6 Vβ domain (compare Figs. 3*B* and 4*C*). Together, this suggests that the folding capabilities of the variable domains from different TCRs vary.

To provide structural insights into the TCR $\alpha\beta$ assembly process that are not amenable to *in vivo* analyses, we performed *in vitro* studies with purified proteins. To this end, we recombinantly expressed the A6 TCR α and β chains (using soluble constructs devoid of their TM regions, denoted $\alpha^{\Delta TM}$ or $\beta^{\Delta TM}$, respectively; Fig. 1*A*) as well as their individual ectodomains and assessed the folding status by CD and NMR spectroscopy. As expected from the $\alpha\beta$TCR crystal structure (Fig. 1*A*) (26, 27), the far-UV CD spectrum of $\beta^{\Delta TM}$ displayed typical characteristics of a protein dominated by β sheet secondary structure; namely, a minimum around 220 nm and a maximum around 200 nm (Fig. 5*A*, *blue tracing*). However, $\beta^{\Delta TM}$ displayed low signal intensities around 200 nm, which is indicative of the presence of unstructured regions. This was even more pronounced for $\alpha^{\Delta TM}$ (Fig. 5*A*, *red tracing*). To further dissect this finding, we individually analyzed the variable and constant domains. In keeping with our *in vivo* studies, the far-UV CD spectrum of Vα (Fig. 5*B*, *green tracing*) was that of a well folded β sheet protein, whereas Cα showed the spectrum of a predominantly unfolded protein (Fig. 5*B*, *red tracing*). We observed a similar behavior for the constituents of the β chain but with the domains switched. Cβ was well folded (Fig. 5*B*, *blue tracing*), whereas Vβ was not amenable to structural studies because of its tendency to aggregate. Therefore, it most likely accounts for the less well folded parts within $\beta^{\Delta TM}$ (compare the spectra in Fig. 5, *A* and *B*). In agreement with our CD data, the ^{1}H-^{15}N TROSY HSQC NMR spectrum of the Cα domain had limited chemical shift dispersion and narrow line widths, indicating fast interconversion of different conformations. It was therefore typical of a disordered protein lacking a defined structure (Fig. 5*C*, *red spectrum*). Of note, the resonances observed for the Cα domain were almost completely superimposable with a subset of signals of the ^{1}H-^{15}N TROSY HSQC spectrum obtained for $\alpha^{\Delta TM}$ (Fig. 5*C*, *black spectrum*), and the remaining, mostly well dispersed resonances superimposed well with the spectrum of Vα (Fig. 5*C*, *green spectrum*). Therefore, also in the context of $\alpha^{\Delta TM}$, Cα appears to be unstructured, whereas Vα is well folded.

Assembly-dependent Folding of the TCR α and β Chains—Taken together, our *in vitro* data show that the A6 TCR α and β chains each comprise one well folded domain (Vα and Cβ, respectively) and one less well folded domain in isolation. Cα appeared to be almost completely unfolded both in isolation and within the $\alpha^{\Delta TM}$ chain. In contrast, Vβ seemed to possess some β sheet structure, at least in the context of the complete $\beta^{\Delta TM}$ chain, as indicated by the presence of more β sheet structure in the CD spectrum of $\beta^{\Delta TM}$ compared with that of $\alpha^{\Delta TM}$ (Fig. 5*A*). *In vivo*, the Vα and Cβ domains of the A6 TCR formed their internal disulfide bridge and only weakly bound to BiP, whereas Cα and Vβ stably bound to BiP and remained reduced (Figs. 3*B* and 4*A*). On the basis of this good agreement between

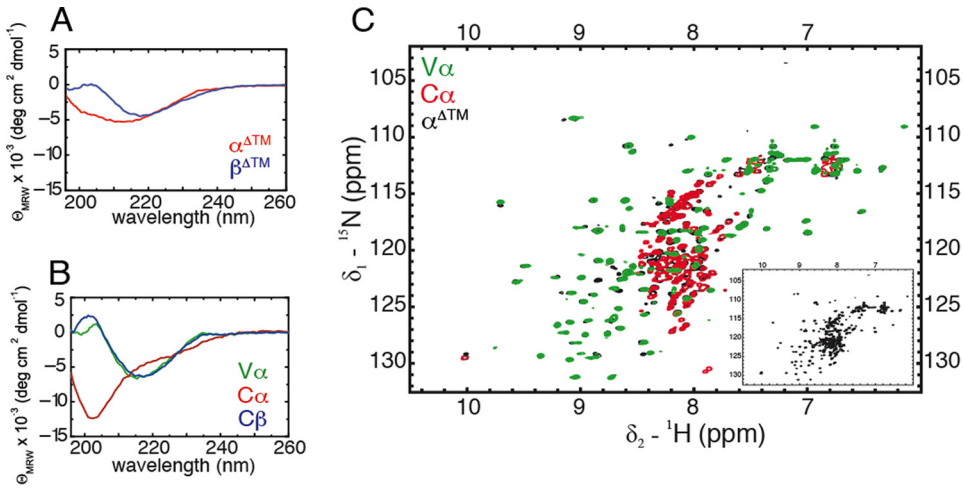

FIGURE 5. **Structural properties of the TCR α/β chains and domains *in vitro*.** *A*, far-UV CD spectra of $\alpha^{\Delta TM}$ (*red*) and $\beta^{\Delta TM}$ (*blue*). *MRW*, mean residue weight. *B*, far-UV CD spectra of Vα (*green*), Cα (*red*), and Cβ (*blue*). Minima around 200 nm are indicative of unstructured regions, whereas β sheet proteins are expected to show a minimum around 220 nm and a maximum around 200 nm. *C*, ^{1}H-^{15}N TROSY HSQC spectra of ^{15}N-labeled $\alpha^{\Delta TM}$ (*black*) overlaid with the spectra of ^{15}N-labeled Vα (*green*) and ^{15}N-labeled Cα (*red*). The *inset* shows the isolated spectrum of ^{15}N-labeled $\alpha^{\Delta TM}$ (*black*). All measurements were performed at 25 °C in PBS, supplemented with 10% D_2O in the case of NMR experiments.

our *in vitro* and *in vivo* data, we used the recombinant proteins to analyze the assembly process of the α and β chains and the concomitant structural changes in more detail. To this end, we performed partial proteolysis experiments on the recombinant proteins. Products were analyzed by both SDS-PAGE and mass spectrometry. Under non-reducing conditions, $\alpha^{\Delta TM}$ migrated as four distinct bands (Fig. 6*A*, *left panel*) that resolved into a single band under reducing conditions (Fig. 6*D*), indicative of disulfide bonding heterogeneity. Partial proteolysis with trypsin rapidly degraded these four species into a single one that we identified by mass spectrometry to be the Vα domain (Fig. 6*A*, *left panel*, and *B*), arguing that Cα causes the disulfide bonding heterogeneity. Cα contains two cysteines, and the flexible stalk of the α chain contains an additional cysteine that forms an interchain disulfide bond with the β chain in the mature receptor (26, 27) (Fig. 1*A*). If all redox species of a three cysteine-containing protein are populated, four species are expected, exactly what we observed. *In vivo*, only a single redox species could be detected (Fig. 4*A*), arguing that this potential for heterogeneity is suppressed in cells. In comparison to the α chain, the β chain was degraded more slowly by trypsin (Fig. 6*A*, *center panel*). All stable fragments contained the Cβ domain (Fig. 6*B*), in agreement with the finding that Vβ is the less well folded domain. When assembled, the αβ heterodimer only populated a single redox species and was very resistant to proteolytic digestion (Fig. 6, *A*–*C*), which indicates assembly-induced folding events in the TCR α and β chains.

To identify minimal elements needed for αβ heterodimerization and concomitant folding events, we assessed the interaction of the α chain with the Cβ domain and, vice versa, of the β chain with the Cα domain. No covalent dimers could be detected in either case (Fig. 6*D*), arguing that interaction of the constant domains depends on the additional presence of the variable domains. NMR spectroscopy supported this finding (Fig. 6*E*). Interestingly, when we used a β chain in which the cysteine residue that forms the interchain disulfide bridge with the α chain was deleted (Fig. 1*A*, $\beta^{\Delta TM,\ \Delta Cys}$), it was still capable of reshuffling the various α chain redox species and led to the predominant population of a single α chain species in $\alpha^{\Delta TM}$ (Fig. 6*D*). This strengthens our conclusion that the β chain induces folding of Cα and that assembly-dependent folding does not depend on the presence of the interchain disulfide bond, which is in agreement with the fact that the αβ interchain disulfide bond is dispensable for TCR transport to the cell surface (42).

Taken together, our data suggest a mechanism of reciprocally induced domain folding upon heterodimerization of the TCR α/β chains. Unfolded domains are specifically recognized by ER chaperones, and their folding is a prerequisite for release from the designated chaperones in the ER environment. Together, this allows ERQC to monitor the proper assembly of functional αβTCRs.

Discussion

How comparable data obtained from *in vitro* analyses are to those from *in vivo* folding studies is a matter of considerable debate. For all proteins analyzed in this study, a very good agreement existed. For domains that appeared well folded *in vitro* (A6 Vα and Cβ), we found evidence of disulfide bridge formation and the absence of binding to the Hsp70 chaperone BiP *in vivo*. Similarly, *in vitro* patterns signifying unfolded/unstructured domains correlated with stable BiP binding and the absence of disulfide bond formation *in vivo* (A6 Cα and Vβ). Binding of calnexin was strongly dependent on membrane integration and could therefore not be assessed easily on a single-domain basis. Of note, even though disulfide bond formation can occur in unfolded proteins *in vitro*, *in vivo* folding and oxidation seem to be coupled more tightly (24, 43, 44).

The good agreement between our *in vitro* and *in vivo* folding data allowed us to use the complementary strengths of these approaches to analyze the structural details underlying ERQC of TCR α/β chain assembly. Our data show that the constant domain of the α chain, Cα, is unfolded and gains structure upon αβ heterodimerization. Before assembling with a β chain, the

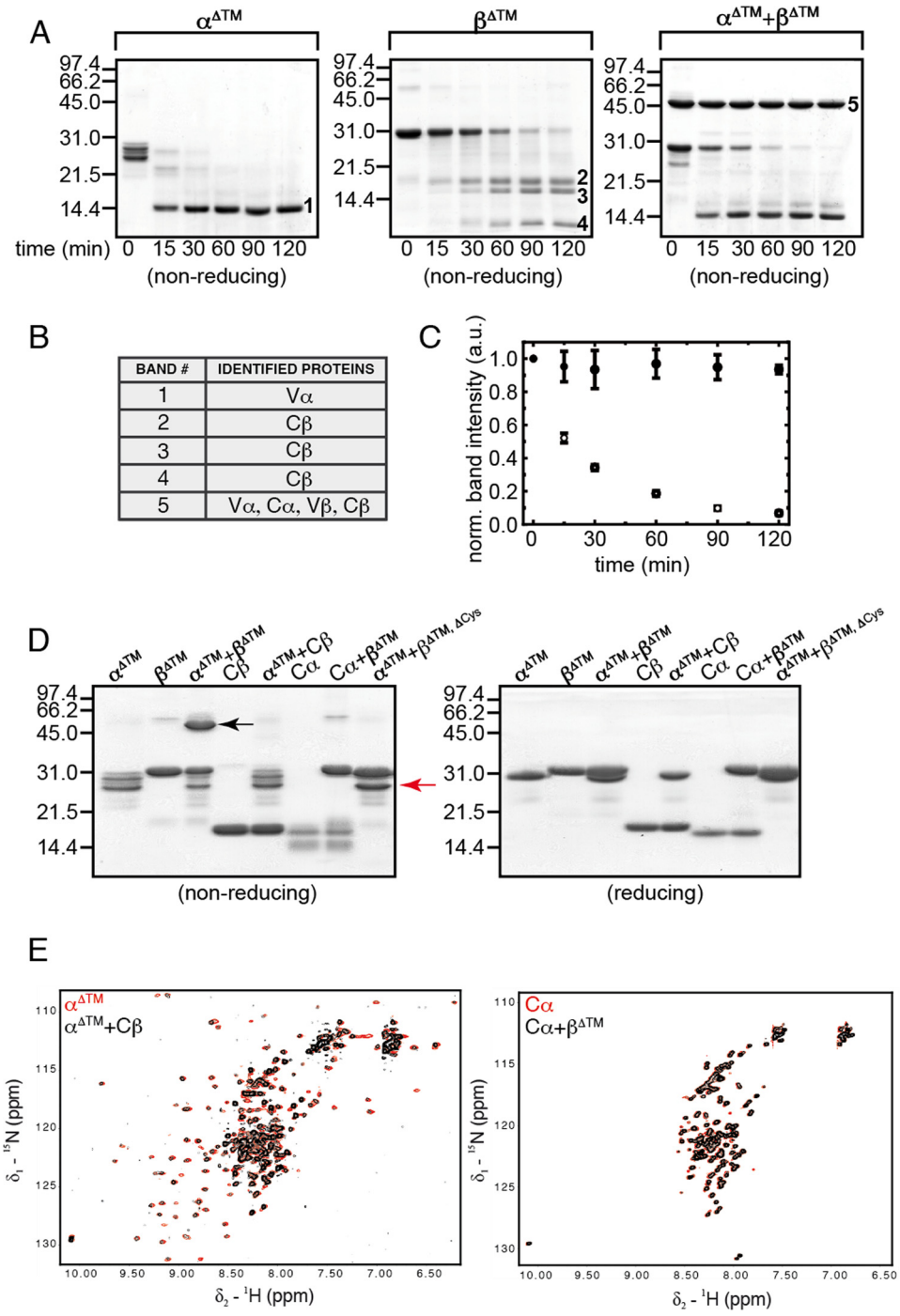

FIGURE 6. **Structural changes within the TCR α and β chains upon interaction and identification of minimal interaction elements.** *A*, partial proteolysis of $\alpha^{\Delta TM}$ or $\beta^{\Delta TM}$ and their covalent heterodimer *in vitro*. Major proteolytic fragments were analyzed by mass spectrometry (indicated with *numbers*). Digestion times with trypsin are shown below the gels. Proteins were analyzed by non-reducing SDS-PAGE. *B*, identified proteins from the proteolytic digest in *A*. *C*, quantification of $\alpha^{\Delta TM}/\beta^{\Delta TM}$ degradation upon trypsin treatment in *A*. *Open symbols* show the sum of the band intensities for the isolated $\alpha^{\Delta TM}$ and $\beta^{\Delta TM}$ chains, and *closed symbols* show the band intensity of the covalent αβ heterodimer ($n = 3$, mean ± S.D.). *norm.*, normalized. *a.u.*, arbitrary units. *D*, disulfide bridge formation was used as a reporter for productive assembly of the different TCR chains and domains. Reactions were carried out in the presence of a GSH/GSSG redox system prior to analysis on non-reducing (*left panel*) or reducing (*right panel*) SDS-PAGE gels. Co-incubated proteins are indicated above the lanes. The αβ heterodimer is marked with a *black arrow*. The most compact $\alpha^{\Delta TM}$ species induced upon co-incubation with $\beta^{\Delta TM, \Delta Cys}$ is marked with a *red arrow*. *E*, *left panel*, superimposition of the ^{1}H-^{15}N TROSY HSQC spectra of the isolated ^{15}N-labeled $\alpha^{\Delta TM}$ chain (*red*) with the ^{15}N-labeled $\alpha^{\Delta TM}$ chain in the presence of unlabeled Cβ (*black*) demonstrates a lack of structural changes upon addition of Cβ. *right panel*, superimposition of the ^{1}H-^{15}N TROSY HSQC spectra of the isolated ^{15}N-labeled Cα domain (*red*) with the ^{15}N-labeled Cα domain in the presence of $\beta^{\Delta TM}$ (*black*) demonstrates the absence of structural changes upon addition of $\beta^{\Delta TM}$. Measurements were performed at 25 °C in PBS supplemented with 10% D_2O with a 2-fold excess of the unlabeled proteins over the ^{15}N-labeled proteins each.

Cα domain therefore provides interaction sites for ER chaperones, BiP and Cnx, allowing recognition of unassembled α-CD3δε trimers. In the case of the β chains analyzed in this study, the Vβ domain is a strong client of BiP, providing a means for retaining β-CD3γε trimers. Of note, even though the HA TCR Vβ domain formed its disulfide bond *in vivo*, it

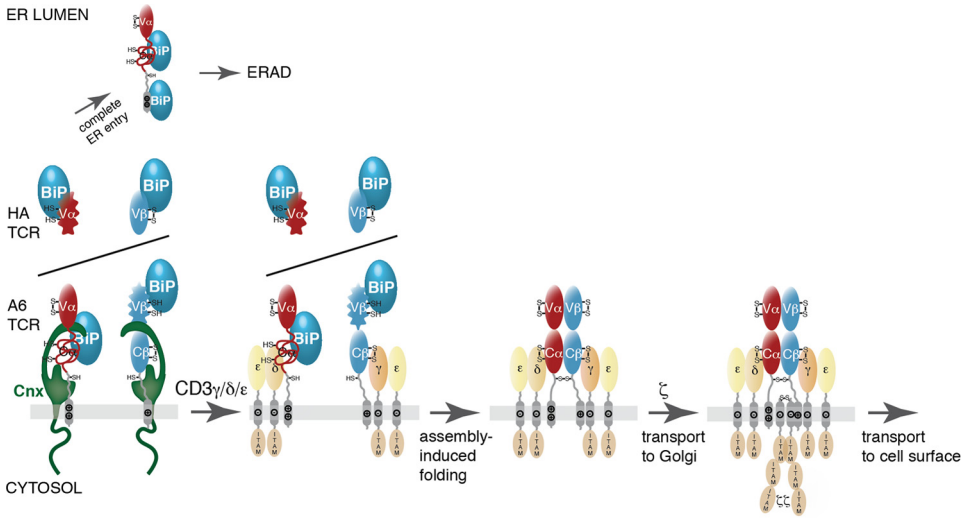

FIGURE 7. **A model for αβTCR assembly control in the cell.** Unassembled clonotypic α and β chains are both Cnx substrates. The α chain comprises either one (Cα) or two (Cα and Vα) incompletely folded domains. The β chain Cβ domain is well folded whereas Vβ, in at least some αβTCRs, is not. All incompletely folded domains provide BiP interaction sites, with particular strong binding to incompletely folded variable domains. Of note, Vβ binds to BiP independently of its capability to form its intradomain disulfide bond. Over time, because of their hydrophilic TM region, unpaired α chains completely enter the ER lumen and are degraded by ER-associated degradation (*ERAD*) (14, 15, 29, 46). Note that αβ heterodimerization should retain the α chain at the membrane but might fail to integrate its TM region if the α-chain is not assembled with the CD3 complex (7, 8, 10). Correctly assembled α-CD3δε and β-CD3γε pairs *en route* to the native receptor, whose interaction with Cnx might be reduced or abolished (32), still provide BiP binding sites in Vβ and, likely, Cα, even though the temporal relationship of Cnx and BiP binding is not entirely clear. Upon αβ heterodimerization, the incompletely folded domains in the clonotypic chains become structured and are therefore released from chaperones. Finally, assembly with ζ dimers in the Golgi allows transport to the cell surface to occur (13, 21, 22, 57).

remained a strong BiP substrate. Therefore, BiP binding sites are present even in an oxidized Vβ domain. This implies that, unlike antibodies, where free light chains (LCs) can be secreted whereas unassembled heavy chains (HCs) are retained, both clonotypic chains of αβTCRs provide a focus of ERQC. This difference becomes biologically meaningful when one keeps in mind that antibody LCs do not have any effector functions whereas antibody HCs do, and TCR α-CD3δε and β-CD3γε trimers might each trigger aberrant signaling when transported to the cell surface (45). ERQC therefore acts on all antibody and TCR components that could be potentially harmful when transported while assembled incompletely. Taken together, only the combined reciprocal folding of both V and C domains upon assembly produces an αβ-CD3γδε$_2$ hexamer that no longer interacts with ER chaperones and can be transported to the Golgi, where ζ_2 homodimers are added to complete the αβTCR. However, each V domain is unique. Our data show that this may cause different folding properties, which indicates some previously unappreciated restrictions on compatible TCR Vα-Vβ pairs and, therefore, the possible T cell repertoire.

The data presented in this study reveal interesting similarities and differences in terms of ERQC mechanisms between the αβTCR and antibodies. For IgG antibodies, the first constant domain (C_H1) of the HC is unfolded while HCs are unpaired and gains structure upon HC-LC assembly. This allows HCs to be retained by BiP in developmentally immature pre-B cells that are not producing LCs and for BiP to be released and antibody secretion to occur in more mature cells that produce LCs (24, 46, 47). Our data indicate, for αβTCRs, that the Cα domain behaves as a similar target of ERQC. Of note, although C_H1 adopts a regular Ig fold when assembled, Cα lacks an entire β strand in its Ig fold and remains flexible even in the αβ heterodimer (26, 27). This might explain why assembly of the TCR constant domains *in vitro* depends on the additional presence of the variable domains, whereas C_H1 can assemble with its cognate partner domain C_L *in vitro* in the absence of the variable regions (46). Another distinction is that IgG assembly primarily relies on the BiP-centered Hsp70 system of the ER (48), whereas the lectins Crt and, in particular, Cnx are major chaperones for the αβTCR (30–32, 49). Cα is the most heavily glycosylated of all αβTCR domains (Fig. 1*A*), which might facilitate Cnx recruitment to this incompletely folded domain and contribute to the relatively weak BiP binding we observed (38, 39).

Interestingly, in the case of antibodies, the unfolded C_H1 domain is found in HCs, which are expressed first during development. In contrast, the incompletely folded Cα domain is found in the TCR α chain, which developmentally corresponds to antibody LCs, and not in the β chain, which is expressed first (50, 51). For both arms of the adaptive immune response, a mechanism exists for transporting a small amount of the chain that is produced first to the surface for signaling. In the case of pre-B cells, this is achieved by the expression of a surrogate light chain (52) that is able to assemble with HCs to relieve them from ER retention (50, 52, 53). Conversely, immature T cells make a pre-TCRα (54). Even though the pre-TCRα lacks a variable region, it is still able to interact with both the Cβ and the Vβ domain (55) to allow surface expression of the β chain. Our data suggest that Cβ is well folded, which might provide a docking site for pre-TCRα, allowing it to induce further folding or shielding of hydrophobic surfaces in Vβ (55) so that BiP is released and the β chain can be expressed on the cell surface of pre-T cells. This provides a rationale for why pre-TCRα needs to interact with both domains to allow the TCR β chain to leave the ER.

Taken together, our study allows us to propose a detailed model for αβTCR assembly control in the cell (Fig. 7). Even though important differences are observed in ERQC mechanisms overseeing the maturation of the clonotypic chains in αβTCRs and antibodies, the functions of both molecules in the immune response demand highly reliable quality control checkpoints prior to transport to the cell surface. To fulfill these requirements, antibodies and TCRs have evolved quality control steps relying on assembly-induced folding. The choice of domains and even on which chains they are found, in terms of the developmental sequence of expression, argues that this critical step in ERQC for immune receptors has arisen twice through convergent evolution.

Author Contributions—M. J. F. and L. M. H. conceived the study. T. M. carried out NMR experiments. All other experiments were performed by M. J. F. and J. B. M. J. F., J. B., T. M., and L. M. H. analyzed the data and wrote the paper.

Acknowledgments—We thank Johannes Buchner, Technische Universität München, for support of several in vitro experiments. We also thank the protein production facility, the Hartwell Center, and the mass spectrometry core of St. Jude Children's Research Hospital for support.

References

1. Braakman, I., and Hebert, D. N. (2013) Protein folding in the endoplasmic reticulum. *Cold Spring Harb. Perspect. Biol.* **5,** a013201
2. Brodsky, J. L., and Skach, W. R. (2011) Protein folding and quality control in the endoplasmic reticulum: recent lessons from yeast and mammalian cell systems. *Curr. Opin. Cell Biol.* **23,** 464–475
3. Smith, M. H., Ploegh, H. L., and Weissman, J. S. (2011) Road to ruin: targeting proteins for degradation in the endoplasmic reticulum. *Science* **334,** 1086–1090
4. Guerriero, C. J., and Brodsky, J. L. (2012) The delicate balance between secreted protein folding and endoplasmic reticulum-associated degradation in human physiology. *Physiol. Rev.* **92,** 537–576
5. Gershenson, A., and Gierasch, L. M. (2011) Protein folding in the cell: challenges and progress. *Curr. Opin. Struct. Biol.* **21,** 32–41
6. Hartl, F. U., and Hayer-Hartl, M. (2009) Converging concepts of protein folding *in vitro* and *in vivo*. *Nat. Struct. Mol. Biol.* **16,** 574–581
7. Bonifacino, J. S., Cosson, P., and Klausner, R. D. (1990) Colocalized transmembrane determinants for ER degradation and subunit assembly explain the intracellular fate of TCR chains. *Cell* **63,** 503–513
8. Call, M. E., Pyrdol, J., Wiedmann, M., and Wucherpfennig, K. W. (2002) The organizing principle in the formation of the T cell receptor-CD3 complex. *Cell* **111,** 967–979
9. Fayadat, L., and Kopito, R. R. (2003) Recognition of a single transmembrane degron by sequential quality control checkpoints. *Mol. Biol. Cell* **14,** 1268–1278
10. Feige, M. J., and Hendershot, L. M. (2013) Quality control of integral membrane proteins by assembly-dependent membrane integration. *Mol. Cell* **51,** 297–309
11. Lippincott-Schwartz, J., Bonifacino, J. S., Yuan, L. C., and Klausner, R. D. (1988) Degradation from the endoplasmic reticulum: disposing of newly synthesized proteins. *Cell* **54,** 209–220
12. Manolios, N., Bonifacino, J. S., and Klausner, R. D. (1990) Transmembrane helical interactions and the assembly of the T cell receptor complex. *Science* **249,** 274–277
13. Minami, Y., Weissman, A. M., Samelson, L. E., and Klausner, R. D. (1987) Building a multichain receptor: synthesis, degradation, and assembly of the T-cell antigen receptor. *Proc. Natl. Acad. Sci. U.S.A.* **84,** 2688–2692
14. Huppa, J. B., and Ploegh, H. L. (1997) The α chain of the T cell antigen receptor is degraded in the cytosol. *Immunity* **7,** 113–122
15. Yu, H., Kaung, G., Kobayashi, S., and Kopito, R. R. (1997) Cytosolic degradation of T-cell receptor α chains by the proteasome. *J. Biol. Chem.* **272,** 20800–20804
16. Klausner, R. D., Lippincott-Schwartz, J., and Bonifacino, J. S. (1990) The T cell antigen receptor: insights into organelle biology. *Annu. Rev. Cell Biol.* **6,** 403–431
17. Call, M. E., and Wucherpfennig, K. W. (2004) Molecular mechanisms for the assembly of the T cell receptor-CD3 complex. *Mol. Immunol.* **40,** 1295–1305
18. Clevers, H., Alarcon, B., Wileman, T., and Terhorst, C. (1988) The T cell receptor/CD3 complex: a dynamic protein ensemble. *Annu. Rev. Immunol.* **6,** 629–662
19. Kearse, K. P., Roberts, J. L., and Singer, A. (1995) TCR α-CD3 δ ϵ association is the initial step in α β dimer formation in murine T cells and is limiting in immature CD4+ CD8+ thymocytes. *Immunity* **2,** 391–399
20. Cosson, P., Lankford, S. P., Bonifacino, J. S., and Klausner, R. D. (1991) Membrane protein association by potential intramembrane charge pairs. *Nature* **351,** 414–416
21. Delgado, P., and Alarcón, B. (2005) An orderly inactivation of intracellular retention signals controls surface expression of the T cell antigen receptor. *J. Exp. Med.* **201,** 555–566
22. Mallabiabarrena, A., Fresno, M., and Alarcón, B. (1992) An endoplasmic reticulum retention signal in the CD3 ϵ chain of the T-cell receptor. *Nature* **357,** 593–596
23. Delaglio, F., Grzesiek, S., Vuister, G. W., Zhu, G., Pfeifer, J., and Bax, A. (1995) NMRPipe: a multidimensional spectral processing system based on UNIX pipes. *J. Biomol. NMR* **6,** 277–293
24. Lee, Y. K., Brewer, J. W., Hellman, R., and Hendershot, L. M. (1999) BiP and immunoglobulin light chain cooperate to control the folding of heavy chain and ensure the fidelity of immunoglobulin assembly. *Mol. Biol. Cell* **10,** 2209–2219
25. Hendershot, L. M., Wei, J. Y., Gaut, J. R., Lawson, B., Freiden, P. J., and Murti, K. G. (1995) *In vivo* expression of mammalian BiP ATPase mutants causes disruption of the endoplasmic reticulum. *Mol. Biol. Cell* **6,** 283–296
26. Garboczi, D. N., Ghosh, P., Utz, U., Fan, Q. R., Biddison, W. E., and Wiley, D. C. (1996) Structure of the complex between human T-cell receptor, viral peptide and HLA-A2. *Nature* **384,** 134–141
27. Garcia, K. C., Degano, M., Stanfield, R. L., Brunmark, A., Jackson, M. R., Peterson, P. A., Teyton, L., and Wilson, I. A. (1996) An αβ T cell receptor structure at 2.5 A and its orientation in the TCR-MHC complex. *Science* **274,** 209–219
28. Hall, C., Berkhout, B., Alarcon, B., Sancho, J., Wileman, T., and Terhorst, C. (1991) Requirements for cell surface expression of the human TCR/CD3 complex in non-T cells. *Int. Immunol.* **3,** 359–368
29. Shin, J., Lee, S., and Strominger, J. L. (1993) Translocation of TCR α chains into the lumen of the endoplasmic reticulum and their degradation. *Science* **259,** 1901–1904
30. Van Leeuwen, J. E., and Kearse, K. P. (1996) The related molecular chaperones calnexin and calreticulin differentially associate with nascent T cell antigen receptor proteins within the endoplasmic reticulum. *J. Biol. Chem.* **271,** 25345–25349
31. Hochstenbach, F., David, V., Watkins, S., and Brenner, M. B. (1992) Endoplasmic reticulum resident protein of 90 kilodaltons associates with the T- and B-cell antigen receptors and major histocompatibility complex antigens during their assembly. *Proc. Natl. Acad. Sci. U.S.A.* **89,** 4734–4738
32. van Leeuwen, J. E., and Kearse, K. P. (1996) Calnexin associates exclusively with individual CD3 δ and T cell antigen receptor (TCR) α proteins containing incompletely trimmed glycans that are not assembled into multisubunit TCR complexes. *J. Biol. Chem.* **271,** 9660–9665
33. Gardner, T. G., Franklin, R. A., Robinson, P. J., Pederson, N. E., Howe, C., and Kearse, K. P. (2000) T cell receptor assembly and expression in the absence of calnexin. *Arch. Biochem. Biophys.* **378,** 182–189
34. Suzuki, C. K., Bonifacino, J. S., Lin, A. Y., Davis, M. M., and Klausner, R. D. (1991) Regulating the retention of T-cell receptor α chain variants within the endoplasmic reticulum: Ca^{2+}-dependent association with BiP. *J. Cell Biol.* **114,** 189–205

35. Behnke, J., and Hendershot, L. M. (2014) The large Hsp70 Grp170 binds to unfolded protein substrates *in vivo* with a regulation distinct from conventional Hsp70s. *J. Biol. Chem.* **289,** 2899–2907
36. Behnke, J., Feige, M. J., and Hendershot, L. M. (2015) BiP and its nucleotide exchange factors Grp170 and Sil1: mechanisms of action and biological functions. *J. Mol. Biol.* **427,** 1589–1608
37. Daniels, R., Kurowski, B., Johnson, A. E., and Hebert, D. N. (2003) *N*-linked glycans direct the cotranslational folding pathway of influenza hemagglutinin. *Mol. Cell* **11,** 79–90
38. Wang, N., Daniels, R., and Hebert, D. N. (2005) The cotranslational maturation of the type I membrane glycoprotein tyrosinase: the heat shock protein 70 system hands off to the lectin-based chaperone system. *Mol. Biol. Cell* **16,** 3740–3752
39. Molinari, M., and Helenius, A. (2000) Chaperone selection during glycoprotein translocation into the endoplasmic reticulum. *Science* **288,** 331–333
40. Braakman, I., Helenius, J., and Helenius, A. (1992) Manipulating disulfide bond formation and protein folding in the endoplasmic reticulum. *EMBO J.* **11,** 1717–1722
41. Hewitt, C. R., Lamb, J. R., Hayball, J., Hill, M., Owen, M. J., and O'Hehir, R. E. (1992) Major histocompatibility complex independent clonal T cell anergy by direct interaction of *Staphylococcus aureus* enterotoxin B with the T cell antigen receptor. *J. Exp. Med.* **175,** 1493–1499
42. Arnaud, J., Huchenq, A., Vernhes, M. C., Caspar-Bauguil, S., Lenfant, F., Sancho, J., Terhorst, C., and Rubin, B. (1997) The interchain disulfide bond between TCR $\alpha\beta$ heterodimers on human T cells is not required for TCR-CD3 membrane expression and signal transduction. *Int. Immunol.* **9,** 615–626
43. Bergman, L. W., and Kuehl, W. M. (1979) Formation of an intrachain disulfide bond on nascent immunoglobulin light chains. *J. Biol. Chem.* **254,** 8869–8876
44. Shimizu, Y., Meunier, L., and Hendershot, L. M. (2009) pERp1 is significantly up-regulated during plasma cell differentiation and contributes to the oxidative folding of immunoglobulin. *Proc. Natl. Acad. Sci. U.S.A.* **106,** 17013–17018
45. Guy, C. S., Vignali, K. M., Temirov, J., Bettini, M. L., Overacre, A. E., Smeltzer, M., Zhang, H., Huppa, J. B., Tsai, Y. H., Lobry, C., Xie, J., Dempsey, P. J., Crawford, H. C., Aifantis, I., Davis, M. M., and Vignali, D. A. (2013) Distinct TCR signaling pathways drive proliferation and cytokine production in T cells. *Nat. Immunol.* **14,** 262–270
46. Feige, M. J., Groscurth, S., Marcinowski, M., Shimizu, Y., Kessler, H., Hendershot, L. M., and Buchner, J. (2009) An unfolded CH1 domain controls the assembly and secretion of IgG antibodies. *Mol. Cell* **34,** 569–579
47. Hendershot, L., Bole, D., Köhler, G., and Kearney, J. F. (1987) Assembly and secretion of heavy chains that do not associate posttranslationally with immunoglobulin heavy chain-binding protein. *J. Cell Biol.* **104,** 761–767
48. Feige, M. J., Hendershot, L. M., and Buchner, J. (2010) How antibodies fold. *Trends Biochem. Sci.* **35,** 189–198
49. David, V., Hochstenbach, F., Rajagopalan, S., and Brenner, M. B. (1993) Interaction with newly synthesized and retained proteins in the endoplasmic reticulum suggests a chaperone function for human integral membrane protein IP90 (calnexin). *J. Biol. Chem.* **268,** 9585–9592
50. Melchers, F. (2005) The pre-B-cell receptor: selector of fitting immunoglobulin heavy chains for the B-cell repertoire. *Nat. Rev. Immunol.* **5,** 578–584
51. von Boehmer, H. (2005) Unique features of the pre-T-cell receptor α-chain: not just a surrogate. *Nat. Rev. Immunol.* **5,** 571–577
52. Pillai, S., and Baltimore, D. (1987) Formation of disulphide-linked μ 2 ω 2 tetramers in pre-B cells by the 18K ω-immunoglobulin light chain. *Nature* **329,** 172–174
53. Minegishi, Y., Hendershot, L. M., and Conley, M. E. (1999) Novel mechanisms control the folding and assembly of λ5/14.1 and VpreB to produce an intact surrogate light chain. *Proc. Natl. Acad. Sci. U.S.A.* **96,** 3041–3046
54. Groettrup, M., Ungewiss, K., Azogui, O., Palacios, R., Owen, M. J., Hayday, A. C., and von Boehmer, H. (1993) A novel disulfide-linked heterodimer on pre-T cells consists of the T cell receptor β chain and a 33 kd glycoprotein. *Cell* **75,** 283–294
55. Pang, S. S., Berry, R., Chen, Z., Kjer-Nielsen, L., Perugini, M. A., King, G. F., Wang, C., Chew, S. H., La Gruta, N. L., Williams, N. K., Beddoe, T., Tiganis, T., Cowieson, N. P., Godfrey, D. I., Purcell, A. W., Wilce, M. C., McCluskey, J., and Rossjohn, J. (2010) The structural basis for autonomous dimerization of the pre-T-cell antigen receptor. *Nature* **467,** 844–848
56. Gascoigne, N. R. (1990) Transport and secretion of truncated T cell receptor β-chain occurs in the absence of association with CD3. *J. Biol. Chem.* **265,** 9296–9301
57. Dietrich, J., Kastrup, J., Lauritsen, J. P., Menné, C., von Bülow, F., and Geisler, C. (1999) TCRζ is transported to and retained in the Golgi apparatus independently of other TCR chains: implications for TCR assembly. *Eur. J. Immunol.* **29,** 1719–1728